

# Virophage control of antarctic algal host–virus dynamics

Sheree Yau<sup>a</sup>, Federico M. Lauro<sup>a</sup>, Matthew Z. DeMaere<sup>a</sup>, Mark V. Brown<sup>a</sup>, Torsten Thomas<sup>a,b</sup>, Mark J. Raftery<sup>c</sup>, Cynthia Andrews-Pfannkoch<sup>d</sup>, Matthew Lewis<sup>d</sup>, Jeffrey M. Hoffman<sup>d</sup>, John A. Gibson<sup>e</sup>, and Ricardo Cavicchioli<sup>a,1</sup>

<sup>a</sup>School of Biotechnology and Biomolecular Sciences, <sup>b</sup>Centre for Marine Bio-Innovation, and <sup>c</sup>Bioanalytical Mass Spectrometry Facility, University of New South Wales, Sydney, New South Wales 2052, Australia; <sup>d</sup>J. Craig Venter Institute, Rockville, MD 20850; and <sup>e</sup>Marine Research Laboratories, Tasmanian Aquaculture and Fisheries Institute, University of Tasmania, Hobart, Tasmania 7001, Australia

Edited\* by Rita R. Colwell, University of Maryland, College Park, MD, and approved March 10, 2011 (received for review December 5, 2010)

Viruses are abundant ubiquitous members of microbial communities and in the marine environment affect population structure and nutrient cycling by infecting and lysing primary producers. Antarctic lakes are microbially dominated ecosystems supporting truncated food webs in which viruses exert a major influence on the microbial loop. Here we report the discovery of a virophage (relative of the recently described Sputnik virophage) that preys on phycodnaviruses that infect prasinophytes (phototrophic algae). By performing metaproteogenomic analysis on samples from Organic Lake, a hypersaline meromictic lake in Antarctica, complete virophage and near-complete phycodnavirus genomes were obtained. By introducing the virophage as an additional predator of a predator–prey dynamic model we determined that the virophage stimulates secondary production through the microbial loop by reducing overall mortality of the host and increasing the frequency of blooms during polar summer light periods. Virophages remained abundant in the lake 2 y later and were represented by populations with a high level of major capsid protein sequence variation (25–100% identity). Virophage signatures were also found in neighboring Ace Lake (in abundance) and in two tropical lakes (hypersaline and fresh), an estuary, and an ocean upwelling site. These findings indicate that virophages regulate host–virus interactions, influence overall carbon flux in Organic Lake, and play previously unrecognized roles in diverse aquatic ecosystems.

metagenomics | metaproteomics | East Antarctica | Vestfold Hills | microbial ecology

It has been known for at least 20 y that viruses frequently infect and lyse marine primary producers, causing up to 70% of cyanobacterial mortality (1, 2). Eukaryotic phytoplankton are preyed upon by large dsDNA phycodnaviruses (PVs), causing bloom termination in globally distributed species (3–6). Elevated levels of dissolved organic carbon (7) and numbers of heterotrophic bacteria (8–10) occur during algal blooms, indicating that viral lysis of eukaryotic algae stimulates secondary production. Viruses also suppress host populations at concentrations below bloom-forming levels, with abundance being controlled by the efficiency and production rates of the infecting viruses (11, 12).

Antarctic lakes are microbially dominated ecosystems supporting few, if any metazoans in the water column (13, 14). In these truncated food webs, viruses are expected to play an increased role in the microbial loop (15). Low-complexity Antarctic lake systems are amenable to whole community-based molecular analyses whereby the role that viruses play in microbial dynamics can be unraveled (14). Attesting to this, a metagenomic study of Lake Linneopolar, West Antarctica uncovered a dominance of eukaryotic viruses and ssDNA viruses previously unknown in aquatic systems (16).

We established a metaproteogenomic program for Organic Lake (68° 27' 23.4" S, 78° 11' 22.6" E), which is located in the Vestfold Hills, East Antarctica, to functionally characterize its microbial community. Organic Lake is a shallow (7 m) hyper-

saline ( $\approx 230$  g L<sup>-1</sup> maximum salinity) meromictic lake with a high concentration of dimethylsulphide ( $\approx 120$   $\mu$ g L<sup>-1</sup>) in its anoxic monimolimnion (17, 18). Water temperature at the surface of the lake can vary from  $-14$  to  $+15$  °C while remaining subzero at depth (19, 20). The lake is eutrophic, with organic material sourced both from autochthonous production and input from penguins and terrestrial algae. The high concentrations of organic material reflect slow breakdown in the highly saline lake water. The salt in the lake was trapped along with the marine biota when the lake was formed because of falling sea level *ca.* 3,000 y B.P. (21, 22). The lake sediment has both low species diversity (Shannon–Weaver diversity: 1.01) and richness (Chao nonparametric index:  $32 \pm 12$ ) (23). Unlike high-latitude lakes, viral abundance has been reported to increase with trophic status (15) and with salinity in Antarctic lakes (24).

Here we report the analysis of the surface water of Organic Lake, highlighting the presence of a relative of the recently described Sputnik virophage, a small eukaryotic virus that requires a helper *Acanthamoeba polyphaga* mimivirus (APMV) to replicate (25). From metagenomic DNA, a complete Organic Lake virophage (OLV) genome was constructed (the second virophage genome to be described), and near-complete genomes of its probable helper Organic Lake phycodnaviruses (OLPVs).

## Results and Discussion

**Dominance of PVs in Organic Lake.** Water samples from Organic Lake were collected December 2006 and November and December 2008 and microbial biomass collected onto 3.0-, 0.8-, and 0.1- $\mu$ m membrane filters as described previously (14). A large proportion of shotgun sequencing reads (96.2%) from the 0.1- $\mu$ m size fraction of the 2006 Organic Lake metagenome (Table S1) had no significant hits to sequences in the RefSeq database (tBLASTx with *e*-value  $< 1.0 \times 10^{-3}$ ; minimum alignment length: 60 bp; minimum identity: 60%). The degree of assembly was high, with 77% of reads forming part of a scaffold, indicating that the sample contained a few abundant taxa of minimal diversity. Forty-five scaffolds were longer than 10 kb; the five longest ranged from 70 to 171 kb. GC content and coverage were used to separate scaffolds into taxonomic groups (Fig. S1). A broad division was evident between low ( $\leq 41\%$ ) and high ( $\geq 51\%$ ) GC scaffolds, suggesting that they constituted two taxonomic groups.

Author contributions: F.M.L., M.V.B., T.T., J.A.G., and R.C. designed research; S.Y., F.M.L., M.Z.D., M.V.B., T.T., J.M.H., and R.C. performed research; M.J.R., C.A.-P., M.L., and J.M.H. contributed new reagents/analytic tools; S.Y., F.M.L., M.Z.D., and M.V.B. analyzed data; and S.Y., F.M.L., and R.C. wrote the paper.

The authors declare no conflict of interest.

\*This Direct Submission article had a prearranged editor.

Data deposition: The sequences reported in this paper have been deposited in the GenBank database [accession nos. HQ704801 (OLV genome), HQ704802 (OLPV-1), HQ704803 (OLPV-2), and HQ704804–HQ704808 (OLPV genomic fragments)].

<sup>1</sup>To whom correspondence should be addressed. E-mail: r.cavicchioli@unsw.edu.au.

This article contains supporting information online at [www.pnas.org/lookup/suppl/doi:10.1073/pnas.1018221108/-DCSupplemental](http://www.pnas.org/lookup/suppl/doi:10.1073/pnas.1018221108/-DCSupplemental).

All scaffolds in the high-GC group that could be assigned contained phage homologs, as did the one exceptional low-GC scaffold. The low coverage in the high-GC group showed that bacteriophages were not abundant in the 0.1- $\mu$ m fraction. These scaffolds were not analyzed further. The low-GC scaffolds with confident assignments contained sequences matching conserved PV or APMV proteins. These PV-related scaffolds constituted 60% of assembled reads, demonstrating that OLPVs were numerically dominant in the 0.1- $\mu$ m fraction. Transmission electron microscopy (TEM) revealed the presence of virus-like particles with the dimensions and structure typical of PVs (Fig. 1A).

Within the low-GC group, scaffolds separated into a high-coverage (>45 $\times$ ) group, including the five longest scaffolds, and a low-coverage (<22 $\times$ ) group. Two of the scaffolds in the high-coverage group and one in the low-coverage group contained the PV marker DNA polymerase B (DPOB). The two-high coverage DPOB share 76% amino acid identity, and both share  $\approx$ 57% identity with the low-coverage DPOB. DPOB is single-copy throughout the nucleo-cytoplasmic large DNA virus (NCLDV) family to which PVs belong (26, 27), demonstrating that the Organic Lake surface waters contained two closely related abundant PV types (DPOB1 and DPOB2) and a more distantly related lower abundance type (DPOB3).

Phylogenetic analysis clustered Organic Lake DPOB with unclassified lytic marine PV isolates that infect the prymnesiophytes *Chrysochromulina ericina* (CeV1) and *Phaeocystis pouchetii* (PpV), the prasinophyte *Pyramimonas orientalis* (PoV) (4, 28), and uncultured marine PVs related to APMV (29, 30) (Fig. 2A and Fig. S2). Because the host range of PVs broadly correlates with DPOB phylogeny (31, 32), OLPV would infect prasinophytes or prymnesiophytes. The most probable host is the prasinophyte *Pyramimonas* (no prymnesiophyte 18S rRNA gene sequences were present in any size fraction of the Organic Lake metagenome) (Fig. S3).

Supporting the presence of more than one PV, pairs of single-copy PV orthologs (ribonucleotide reductase  $\alpha$  and  $\beta$  subunits,

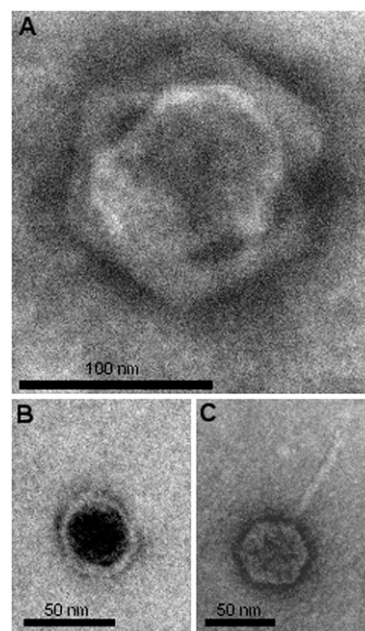


**Fig. 1.** Transmission electron micrographs of negatively stained virus-like particles from Organic Lake. (A) Virus-like particles resembling the size and morphology of PVs, (B) Sputnik virophage, and (C) bacteriophages.

VV A32R virion packaging helicase, PBCV1 A482R-like putative transcription factor, VV D5 ATPase, and VLTF2 family transcription factor) were identified in the high-coverage scaffolds that shared an average of 81% amino acid identity. On the basis of the positions of single-copy genes on the scaffolds and the percentage identity between them, the high-coverage scaffolds were grouped into two strains designated OLPV-1 and

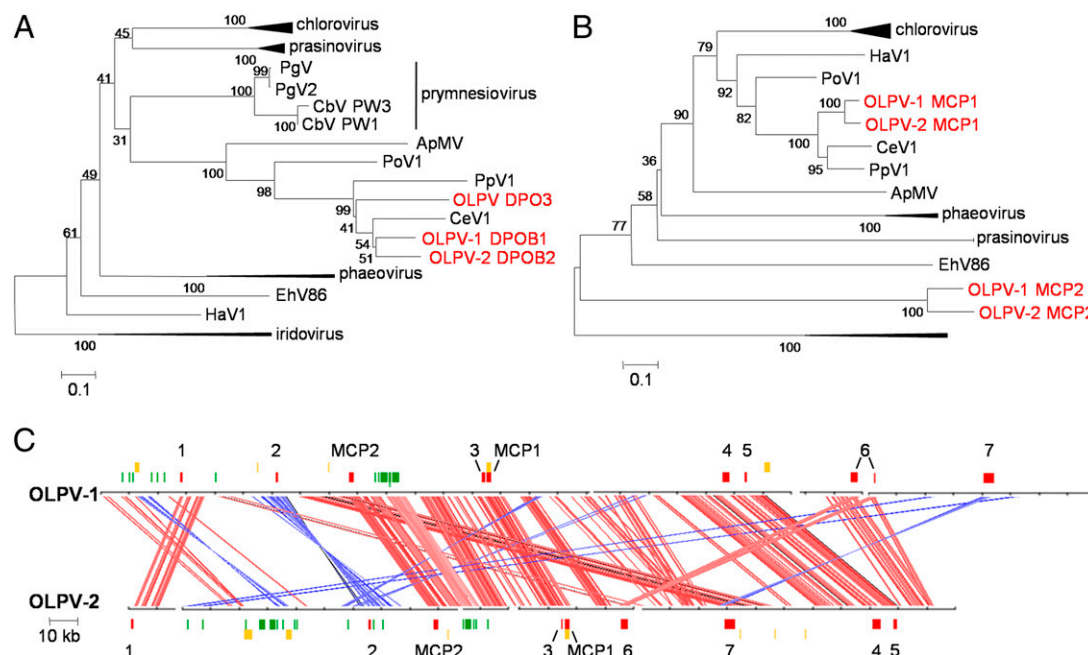


**Fig. 2.** Phylogeny and genomic maps of OLPVs. Neighbor-joining tree of B family DNA polymerase (A) and MCP (B) sequences of OLPV, and NCLDV sequences from GenBank. (C) Maps of OLPV-1 and OLPV-2 scaffolds and comparison of the location of genes; single-copy conserved orthologs and MCP (red); regions with identity to OLV (green); proteins identified in the metaproteome (yellow); ribosomal nucleotide reductase  $\beta$  (1), VV A32 packaging ATPase (2), VV VLTF3 transcription factor (3), VV D5 replicative helicase (4), PBCV-1 A482R-like putative transcription factor (5), ribonucleotide reductase  $\alpha$  (6), and DPOB (7). Lines connect homologous regions between OLPV-1 and OLPV-2 scaffolds in the same orientation (red) and reverse orientation (blue).

OLPV-2, according to their DPOB phylogeny (Fig. 2A and Fig. S2). The remaining high-coverage scaffolds were assigned to either strain, resulting in two near-complete genomes of  $\approx 300$  kb each (Fig. 2C) that are within the range of other sequenced PV genomes (155–407 kb). In addition, several OLPV genomic fragments contained PV homologs in high-coverage scaffolds that could not be confidently assigned to either strain.

Both OLPV strains contain a PpV-like major capsid protein (MCP) designated MCP1 and another unique MCP designated MCP2 (Fig. 2B and Fig. S4). Both OLPV MCP1s were identified in the metaproteome (Fig. 2C and Table S2), but MCP2 was not. In addition to MCPs, the metaproteome contained a range of abundant structural proteins and others more likely to be packaged in the virion (e.g., chaperone) that were expressed by OLPV-1, OLPV-2, and/or an OLPV genomic fragment (Fig. 2C and Table S2). These data suggest that MCP1 is the major structural protein and that both OLPV-1 and OLPV-2 were in a productive cycle in the lake at the time of sampling.

**Complete Genome of an OLV.** Sputnik is a small (50-nm) icosahedral satellite virus of mamavirus (a unique strain of APMV). It was termed a “virophage” because coinfection with Sputnik is deleterious to the mamavirus, resulting in abnormal virions and a decrease in mamavirus infectivity (25). One 28-kb scaffold in the low-GC high-coverage group had six of 38 predicted proteins homologous to Sputnik virophage proteins (Fig. 3 and Table S3) and one PV homolog. The scaffold had a low GC content ( $\approx 30\%$ ), similar to the Sputnik genome, and was larger in size (28 kb vs. 18 kb for Sputnik). Using PCR and sequencing, the scaffold was found to represent a complete circular virophage genome (the Sputnik genome is also circular). Virus-like particles resembling Sputnik in size and morphology were identified by TEM (Fig. 1B).

Sputnik homologs present in the Organic Lake scaffold included the V20 MCP, V3 DNA packaging ATPase, V13 putative DNA polymerase/primase, and others of unknown function (V9, V18, V21, and V32) (Fig. 3 and Table S3). The OLV is distinct to Sputnik because proteins share 27–42% amino acid identity

(28% MCP identity). OLV proteins include OLV9, the homolog of Sputnik V20 MCP, and OLV8, a fusion of the uncharacterized V18 and minor virion protein V19 from Sputnik (Fig. 3 and Table S3). The large number of homologs, including genes that fulfill essential functions in Sputnik (V20, V3, and V13), indicates that OLV and Sputnik have physiological similarities.

**Gene Exchange Between Virophage and PVs.** Because PVs are related to APMV (27) and are abundant in Organic Lake, it stands to reason that OLPV is the helper of OLV. In the OLV genome, OLV12 is a Chlorella virus-derived gene, indicating that gene exchange has occurred between OLV and PVs (the function of OLV12 is discussed below). Similar observations were made for Sputnik, which carries four genes (V6, V7, V12, and V13) in common with the mamavirus, indicative of gene exchange between the viruses and possible coevolution (25). Because the V6, V7, V12, and V13 proteins have been associated with virophage-helper specificity, we reasoned that the functional analogs in OLV would have highest identity to proteins from its helper virus rather than Sputnik.

By comparing OLV and OLPV, a 7,408-bp region was identified in OLV encoding six proteins (OLV17–22) with identity (32–65%) to sequences in both OLPV-1 and OLPV-2 (Fig. 2C, Fig. S5, and Table S3). OLV20 and OLV13 are collagen triple-helix-repeat-containing proteins, analogous to Sputnik collagen-like proteins (V6 and V7) involved in protein–protein interactions in the APMV virus factory. Sputnik can replicate with either mamavirus or APMV as a helper, although coinfection rates are higher with the mamavirus. V6 is the only protein with higher identity (69%) to mamavirus than APMV (42%) (25). Because OLV20 has equivalent identity (63%) with OLPV-1 and OLPV-2, it seems that OLV may be capable of interacting with both OLPV strains. OLV22, also within the conserved region, is a 141-aa protein of unknown function that only matches sequences from OLPV and the Global Ocean Sampling (GOS) expedition (Table S3). Similar to OLV22, Sputnik V12 is a small protein (152 aa) of unknown function with high identity to APMV, and both may mediate a specific helper–virophage in-

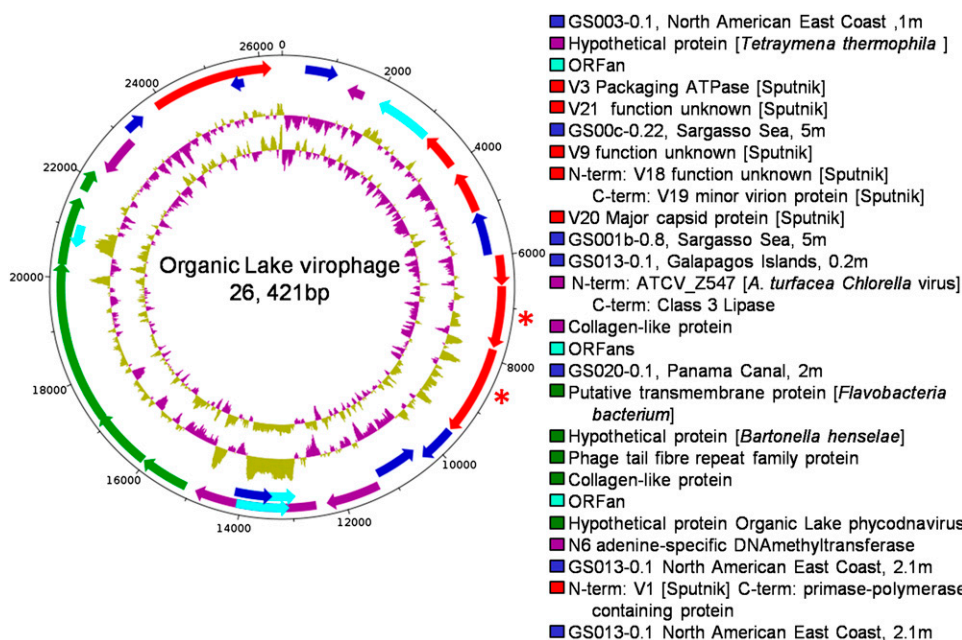


**Fig. 3.** Genomic map of OLV. From the outside in, circles represent (i) predicted coding sequences on the forward strand, (ii) predicted coding sequences on the reverse strand, (iii) GC skew, and (iv) GC plot. Predicted coding sequences are colored: Sputnik homologs (red), OLPV homologs (green), non-Sputnik National Center for Biotechnology Information nonredundant homologs (purple), GOS peptide database homologs (blue), and ORFan (cyan). Sequences identified in the metaproteome are marked with an asterisk. Descriptions of the predicted coding sequences from both strands are shown clockwise from position zero.



teraction. Other genes in this region of OLV can be mapped to OLPV, including a putative transmembrane protein (OLV17) and paralogous phage tail fiber repeat containing proteins OLV18 and OLV19. Analogous to the collagen-like proteins, OLV19 and OLV20 probably facilitate interactions between helper and virophage.

OLV12 (which is unique to OLV) consists of a C-terminal domain present in conserved hypothetical *Chlorella* virus proteins and an N-terminal domain most closely related to class 3 lipases that may confer OLV selectivity to a PV. OLV12 may function similarly to the Sputnik V15 membrane protein in modifying the APMV membrane (25). The Sputnik V13 consists of a primase domain and SF3 helicase domain related to NCLDV homologs, involved in DNA replication. The helicase domain of OLV25 and V13 are similar, although the primase domain is more similar to a protein from *Ostreococcus lucimarinus*, implying a past association of OLV with a prasinophyte alga host.

Genes unique to OLV point to adaptations specific to its helper–host system. Most notably, OLV possesses a N6 adenine-specific DNA methyltransferase, as does OLPV. In OLPV-1, genes for a bacterial type I restriction modification system are adjacent to a gene encoding a type I methylase-S target recognition domain protein and upstream of a DNA helicase distantly related to type III restriction endonuclease subunits. A large number of *Chlorella* virus genomes have both 5mC and 6mA methylation (33), and several contain functional restriction modification systems (34). The prototype *Chlorella* virus PbCV-1

possesses restriction endonucleases packaged in the virion for degrading host DNA soon after infection (35). In contrast to OLV/OLPV, DNA methyltransferases are absent in both Sputnik and APMV, indicating that the N6 adenine-specific DNA methyltransferase has been selected in OLV to reduce endonucleolytic attack mediated by OLPV.

**Role of Virophage in Algal Host–PV Dynamics.** The presence of the virophage adds an additional consideration to the microbial loop dynamics. In batch amoeba cultures, coinfection of amoeba with APMV and Sputnik causes a 70% decrease in infective APMV particles and a threefold decrease in lysis (25). To test how OLV affects OLPV and host population dynamics, we modeled the OLV as an additional predator of a predator in a Lotka–Volterra simulation (Fig. 4). In the model, the effect of virophage is robust, with equilibrium solutions across a wide range of parameter values (Fig. 4 shows one equilibrium solution). By decreasing the number of infective OLPVs, the presence of OLV shortens the recovery time of the host population (Fig. 4C) and shifts the orbit away from the axis (Fig. 4D). The model reveals that the virophage stimulates the flux of secondary production through the microbial loop by reducing overall mortality of the host algal cell after a bloom and by increasing the frequency of blooms during the summer light periods. Antarctic lake systems have evolved mechanisms to cope with long light–dark cycles (14) and shortened trophic chains. In Organic Lake and similar systems, a decrease in PV virulence may be instrumental in maintaining stability of the microbial food web.

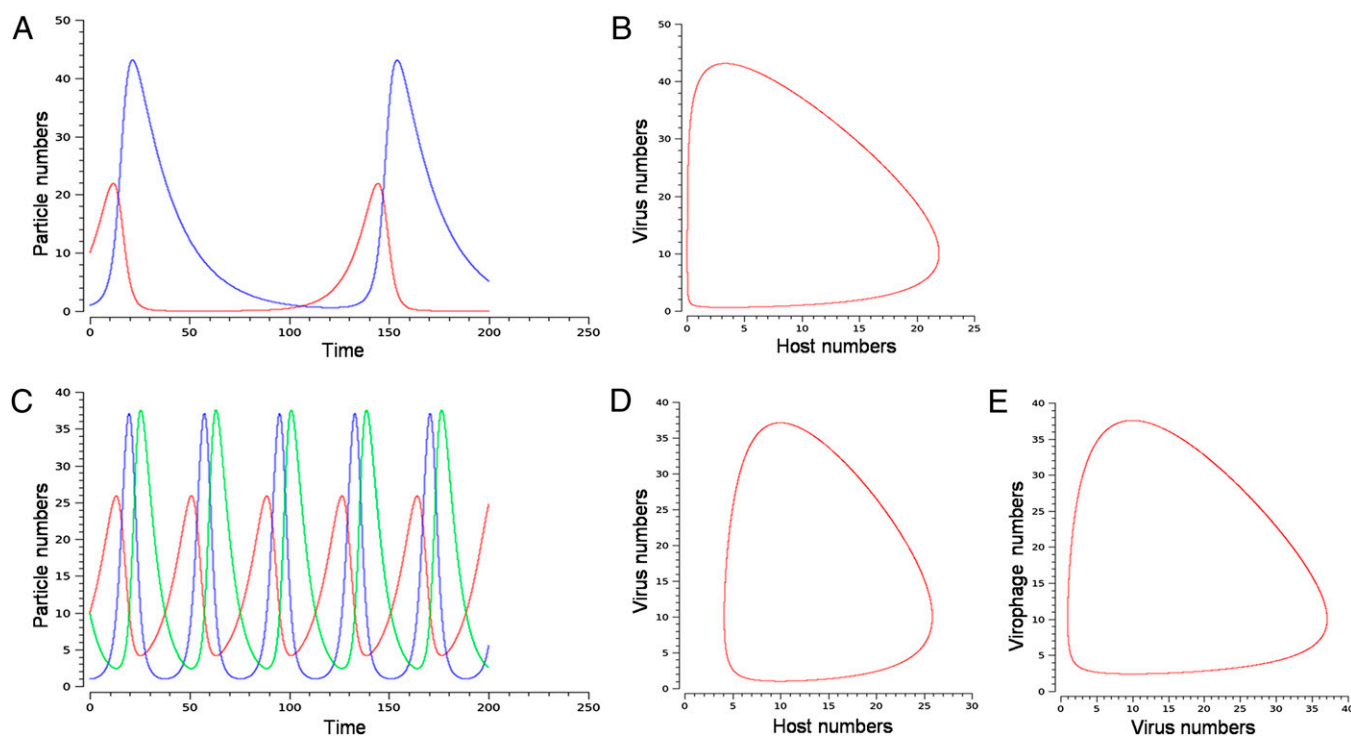


**Fig. 4.** Extended Lotka–Volterra model of host–OLPV–OLV population dynamics. The classic Lotka–Volterra model (37) is based on a pair of first-order, nonlinear, differential equations that can be used to describe the periodic oscillation of the populations of a predator and its prey (38). The extended model shown is based on three equations describing the interactions of host (prey), virus (predator), and virophage (predator of predator) interactions. (A) Time course of host (red line) and virus (blue line) populations. (B) Orbit plot between host and OLPV populations in the absence of OLV, with the host and OLPV populations approaching zero during an equilibrium cycle. (C) Time course describing the effect of the addition of OLV (green line) on OLPV–host population dynamics, resulting in a higher minimal number of hosts and OLPVs (D) compared with in the absence of OLV (B). The orbit plot of OLPV and OLV is also shown (E). The model shows that (independent of the parameters used) although the absolute number of hosts does not increase greatly as a result of OLV preying on OLPV, the frequency of host blooms increases in the presence of OLV. The increased frequency of blooms would increase secondary production (from lysed hosts) and hence overall carbon flux through the system. The increased turnover in the microbial loop during the extended light periods of the polar summer may help to maintain microbial populations in the lake.

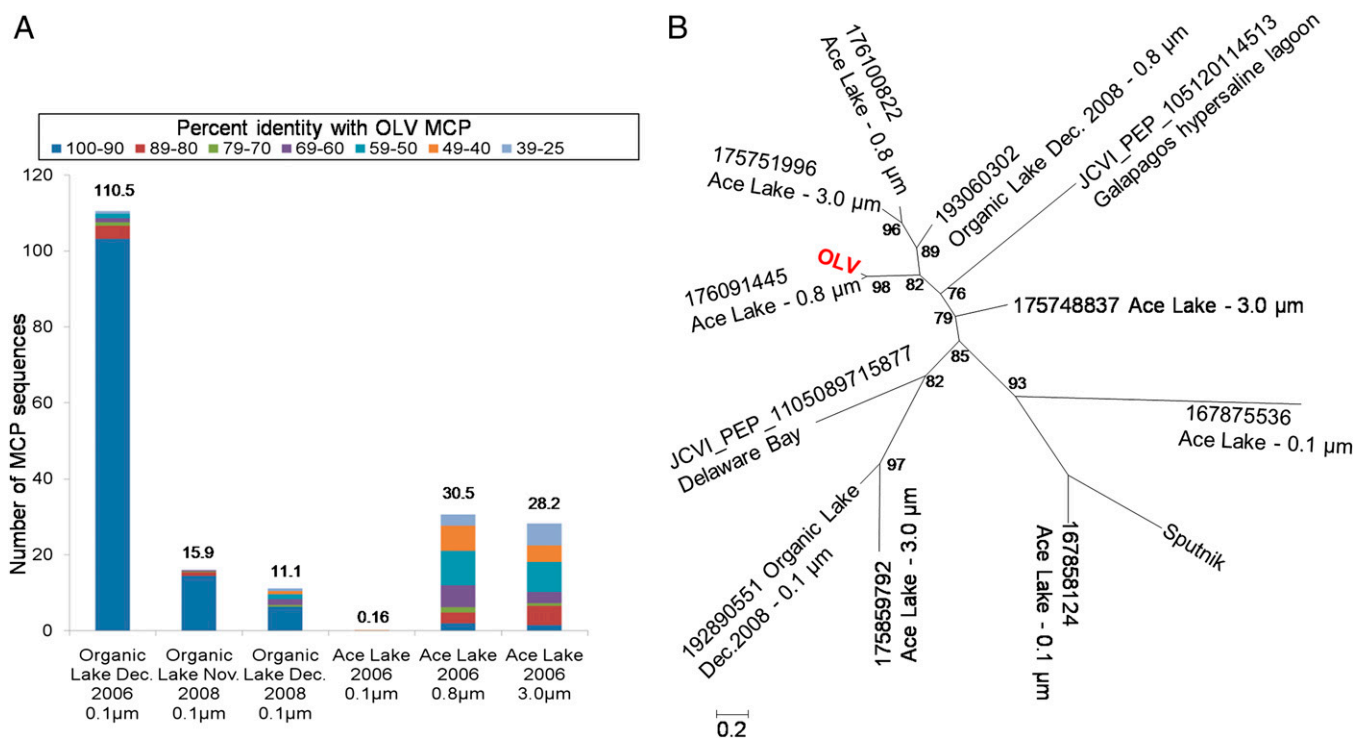


**Fig. 5.** Abundance and diversity of virophage capsid proteins in environmental samples. (A) Number of ORFs from metagenomic reads that match to OLV MCP (BLASTp e-value cutoff  $1e-5$ , abundance normalized to 100,000), and the proportion of virophage capsid types, for the Organic Lake 0.1-μm and Ace Lake 0.1-, 0.8-, and 3.0-μm fractions. (B) Maximum likelihood tree of a conserved 103-aa region of the MCP from Organic Lake, Ace Lake and GOS metagenome data, and Sputnik genome.

**Ecological Relevance of Virophages in Aquatic Systems.** Metagenomic analysis of Organic Lake samples taken 2 y later in November (when the lake was ice-covered) and December 2008 (partially ice-free) revealed sequences with 99% amino acid identity to OLV MCP, indicating persistence of OLV in the ecosystem (Fig. 5 and Table S4). In addition, sequences with lower identity (25–90%) were detected, particularly in December, demonstrating that OLVs are highly diverse but OLV remained the dominant type.

From surface water samples of nearby Ace Lake (meromictic, surface 2% salinity), a large number of sequences were obtained that matched both the OLV MCP (Fig. 5 and Table S4) and PVs (14). All Ace Lake size fractions contained matches to OLV MCP, some with high identity (80–100%) and the majority with greater variation (25–80% identity) (Fig. 5 and Table S4). In contrast to Organic Lake, where the largest number of matches was to the 0.1-μm size fraction, the majority of Ace Lake sequences were from the larger fractions (Fig. 5 and Table S4). This indicates that the Ace Lake virophages were associated with host cells during sampling or possibly with helper viruses that are larger than the OLPVs.

Extending the OLV MCP search to the GOS data revealed matches (25–28% identity) to sequences from the hypersaline Punta Cormorant Lagoon (Floreana Island, Galapagos), an oceanic upwelling near Fernandina Island (Galapagos), Delaware Bay estuary (New Jersey, United States), and freshwater Lake Gatun (Panama) (Table S4). The phylogenetic analysis of a conserved 103-aa region of the MCPs revealed a number of clusters, with Sputnik clustering with virophage sequences from Ace Lake that had low identity (22%) to OLV MCP (Fig. 5 and Fig. S4). To improve searches for virophages and better understand their physiology and evolution, it will be valuable to target more genomes (e.g., the Ace Lake 167858124 relative with 40% MCP identity to Sputnik) and determine which genes are core to virophages and what relationship exists between genome complement and MCP identity.

In view of the implications of the virophage modeling (Fig. 4), the abundance and persistence of OLV in Organic Lake (Fig. 5 and Table S4), and the presence of diverse virophage signatures in a variety of lake systems (fresh to hypersaline), an estuary, an ocean upwelling site, and a water cooling tower (Sputnik), our study indicates that numerous types of virophages exist and play a previously unrecognized role in regulating host–virus interactions and influencing ecosystem function in aquatic environments.

## Materials and Methods

Water samples from Organic Lake were collected December 2006 and November and December 2008, and microbial biomass was collected onto 3.0-, 0.8-, and 0.1-μm membrane filters as described previously (14, 36). DNA extraction, sequencing, phylogenetic analyses, generation of metagenomic assemblies and annotation of OLPV and OLV mosaic genomes, and protein extraction and metaproteomic analyses were performed as previously described (14, 36). Unfiltered Organic Lake water samples from 2006 were fixed in formalin 1% (vol/vol), negatively stained, and visualized by TEM for VLPs. A modified Lotka–Volterra model was used to describe algal host, virus, and virophage dynamics, on the basis of approaches previously described (14). Full details are provided in *SI Materials and Methods*.

**ACKNOWLEDGMENTS.** We thank Craig Venter, John Bowman, Louise (Cromer) Newman, Anthony Hull, John Rich, and Martin Riddle for providing helpful discussion and logistical support associated with the Antarctic expedition; Lisa Ziegler for discussion about marine viruses; Intersect (and in particular Joachim Mai) for technical support for computing infrastructure and software development; and Jenny Norman from the University of New South Wales Electron Microscopy Unit for assistance in generating images. Mass spectrometric results were obtained at the Bioanalytical Mass Spectrometry Facility within the Analytical Centre of the University of New South Wales. This work was undertaken using infrastructure provided by New South Wales Government co-investment in the National Collaborative Research Infrastructure Scheme. Subsidized access to this facility is gratefully acknowledged. This work was supported by the Australian Research Council and the Australian Antarctic Division. Funding for sequencing was provided by the Gordon and Betty Moore Foundation to the J. Craig Venter Institute.

1. Proctor LM, Fuhrman JA (1990) Viral mortality of marine bacteria and cyanobacteria. *Nature* 343:60–62.
2. Suttle CA, Chan AM, Cottrell MT (1990) Infection of phytoplankton by viruses and reduction of primary productivity. *Nature* 347:467–469.
3. Nagasaki K, Ando M, Imai I, Itakura S, Ishida Y (1996) Virus-like particles in *Heterosigma akashiwo* (Raphidophyceae): A possible red tide disintegration mechanism. *Mar Biol* 119:307–312.
4. Jacobsen A (1996) Isolation and characterization of a virus infecting *Phaeocystis pouchetii* (Prymnesiophyceae). *J Phycol* 32:923–927.
5. Wilson WH, et al. (2002) Isolation of viruses responsible for the demise of an *Emiliania huxleyi* bloom in the English Channel. *J Mar Biol Assoc U K* 82:369–377.
6. Martinez JM, Schroeder DC, Larsen A, Bratbak G, Wilson WH (2007) Molecular dynamics of *Emiliania huxleyi* and cooccurring viruses during two separate mesocosm studies. *Appl Environ Microbiol* 73:554–562.
7. Eberlein K, Leal MT, Hammer KD, Hickel W (1985) Dissolved organic substances during a *Phaeocystis pouchetii* bloom in the German Bight (North Sea). *Mar Biol* 89:311–316.
8. Davidson AT, Marchant HJ (1992) Protist abundance and carbon concentration during a *Phaeocystis*-dominated bloom at an Antarctic coastal site. *Polar Biol* 12:387–395.
9. Castberg T, et al. (2001) Microbial population dynamics and diversity during a bloom of the marine coccolithophorid *Emiliania huxleyi* (Haptophyta). *Mar Ecol Prog Ser* 221:39–46.
10. Bratbak G, Jacobsen A, Haldal M (1998) Viral lysis of *Phaeocystis pouchetii* and bacterial secondary production. *Aquat Microb Ecol* 16:11–16.
11. Larsen A, et al. (2001) Population dynamics and diversity of phytoplankton, bacteria and viruses in a seawater enclosure. *Mar Ecol Prog Ser* 221:47–57.
12. Bouvier T, del Giorgio PA (2007) Key role of selective viral-induced mortality in determining marine bacterial community composition. *Environ Microbiol* 9:287–297.
13. Laybourn-Parry J (1997) *Ecosystem Processes in Antarctic Ice-free Landscapes*, eds Lyons WB, Howard-Williams C, Hawes I (Balkema, Rotterdam, The Netherlands), pp 231–240.
14. Lauro FM, et al. (2010) An integrative study of a meromictic lake ecosystem in Antarctica. *ISME J*, 10.1038/ismej.2010.185.
15. Madan NJ, Marshall WA, Laybourn-Parry J (2005) Virus and microbial loop dynamics over an annual cycle in three contrasting Antarctic lakes. *Freshw Biol* 50:1291–1300.
16. López-Bueno A, et al. (2009) High diversity of the viral community from an Antarctic lake. *Science* 326:858–861.
17. Gibson JAE, Garrick RC, Franzmann PD, Deprez PP, Burton HR (1991) Reduced sulfur gases in saline lakes of the Vestfold Hills, Antarctica. *Palaeogeogr Palaeoclimatol Palaeoecol* 84:131–140.
18. Roberts NJ, Burton HR, Pitson GA (1993) Volatile organic compounds from Organic Lake, an Antarctic, hypersaline, meromictic lake. *Antarct Sci* 5:361–366.
19. Franzman PD, Deprez PP, Burton HR, van den Hoff J (1987) Limnology of Organic Lake, Antarctica, a meromictic lake that contains high concentrations of dimethyl sulfide. *Aust J Freshwater Res* 38:409–417.
20. Gibson JAE (1999) The meromictic lakes and stratified marine basins of the Vestfold Hills, East Antarctica. *Antarct Sci* 11:175–192.
21. Zwartz D, Bird M, Stone J, Lambeck K (1998) Holocene sea-level change and ice-sheet history in the Vestfold Hills, East Antarctica. *Earth Planet Sci Lett* 155:131–145.
22. Bird MI, Chiva AR, Radnell CJ, Burton HR (1991) Sedimentological and stable-isotope evolution of lakes in the Vestfold Hills, Antarctica. *Palaeogeogr Palaeoclimatol Palaeoecol* 84:109–130.
23. Bowman JP, McCammon SA, Rea SM, McMeekin TA (2000) The microbial composition of three limnologically disparate hypersaline Antarctic lakes. *FEMS Microbiol Lett* 183: 81–88.
24. Laybourn-Parry J, Hofer JS, Sommaruga R (2001) Viruses in the plankton of freshwater and saline Antarctic lakes. *Freshw Biol* 46:1279–1287.
25. La Scola B, et al. (2008) The virophage as a unique parasite of the giant mimivirus. *Nature* 455:100–104.
26. Iyer LM, Aravind L, Koonin EV (2001) Common origin of four diverse families of large eukaryotic DNA viruses. *J Virol* 75:11720–11734.
27. Iyer LM, Balaji S, Koonin EV, Aravind L (2006) Evolutionary genomics of nucleocytoplasmic large DNA viruses. *Virus Res* 117:156–184.
28. Sandaa RA, Haldal M, Castberg T, Thyraug R, Bratbak G (2001) Isolation and characterization of two viruses with large genome size infecting *Chrysochromulina ericina* (Prymnesiophyceae) and *Pyramimonas orientalis* (Prasinophyceae). *Virology* 290:272–280.
29. Monier A, et al. (2008) Marine mimivirus relatives are probably large algal viruses. *Virology* 379:1–12.
30. Monier A, Claverie JM, Ogata H (2008) Taxonomic distribution of large DNA viruses in the sea. *Genome Biol* 9:R106.
31. Nagasaki K, Shirai Y, Tomaru Y, Nishida K, Pietrovski S (2005) Algal viruses with distinct intraspecies host specificities include identical intein elements. *Appl Environ Microbiol* 71:3599–3607.
32. Larsen JB, Larsen A, Bratbak G, Sandaa RA (2008) Phylogenetic analysis of members of the *Phycodnaviridae* virus family, using amplified fragments of the major capsid protein gene. *Appl Environ Microbiol* 74:3048–3057.
33. Van Etten JL, Lane LC, Meints RH (1991) Viruses and viruslike particles of eukaryotic algae. *Microbiol Rev* 55:586–620.
34. Nelson M, Zhang Y, Van Etten JL (1993) DNA methyltransferases and DNA site-specific endonucleases encoded by chloroviruses. *DNA Methylation: Molecular Biology and Biological Significance*, eds Jost JP, Saluz HP (Birkhäuser, Basel, Switzerland), pp 186–211.
35. Agarkova IV, Dunigan DD, Van Etten JL (2006) Virion-associated restriction endonucleases of chloroviruses. *J Virol* 80:8114–8123.
36. Ng C, et al. (2010) Metaproteogenomic analysis of a dominant green sulfur bacterium from Ace Lake, Antarctica. *ISME J* 4:1002–1019.
37. Lotka AJ (1910) Contribution to the theory of periodic reaction. *J Phys Chem* 14: 271–274.
38. Volterra V (1926) Variazioni e fluttuazioni del numero d'individui in specie animali conviventi. *Mem Acad Lincei Roma* 2:31–113.